RSC Advances

PAPER

View Article Online
View Journal | View Issue

Cite this: *RSC Adv.*, 2015, **5**, 31392

Controlled assembly of hybrid architectures based on carboxylic acid ligands and $[(O_3PCH_2PO_3)Mo_6O_{22}]^{12-}$†

Xiaopeng Sun, Donghui Yang, Gaigai Wang, Zhijie Liang, Pengtao Ma, Jingping Wang* and Jingyang Niu*

Received 31st January 2015
Accepted 19th March 2015

DOI: 10.1039/c5ra01955a

www.rsc.org/advances

The nature of carboxylic acid has a profound effect on constructing POM-based architectures. With different carboxylic acid ligands, three novel diphosphonate-containing compounds have been synthesized and further investigated by elemental analyses, single-crystal X-ray diffraction, IR spectroscopy, UV-vis spectroscopy, X-ray powder diffraction (XRPD), ^{31}P NMR spectroscopy, cyclic voltammetric behavior and thermogravimetric (TG) analyses. $[(HO_3PCH_2PO_3)Mo_6O_{18}(O_2CC_6H_4OH)_2]^{5-}$ (**1a**) shows a ring-shaped cluster with a $\{Mo_6\}$ plane framework. $[\{(HO_3PCH_2PO_3)Mo_6O_{18}(CH_3CO_2)_2\}_2Na_2(H_2O)_2]^{8-}$ (**2a**) is a reverse symmetrical "crown-type" structure and the subunits are linked by two Na–O(1W)–Na bridges. The polyanion $[\{(O_3PCH_2PO_3)(Mo_6O_{18}(H_2O)_2)(O_2CCH_2CO_2)\}_2(Mo_2O_5)_2(\mu_3\text{-}O)_2]^{12-}$ (**3a**) appears as an "S-shaped" structure with a centre of inversion.

Introduction

The design and synthesis of polyoxometalates (POMs) have gained increasing attention not only for their molecular and electronic structural diversity, but also because of their interesting properties in different fields such as catalysis, magnetism, materials science, optics, biology and medicine.[1–8] Recently, a great deal of research from different groups has been aimed at the functionalization of polyoxomolybdate with organic or organometallic ligands. The prospect of POM-based hybrid materials with novel synergistic effects, exceeding tunable properties and convenience for processability is brilliant.[9] The covalent binding of organic groups onto POMs may open up a doorway to new classes of POM-based hybrid materials, which combine the intrinsic properties of POMs and organic components. As a matter of fact, interaction of POMs with carboxylic acid ligands has also been synthesized and characterized,[10] which leads to a large number of functionalized species. For instance, $\{Mo_6O_{18}\}$,[11] $\{Mo_{12}O_{46}\}$,[12] $\{Mo_2O_4\}$,[13] and $\{Mo_{2n}O_{2n}S_{2n}(OH)\}_{2n}$.[14] Meanwhile, a part of diphosphates that generally formularized as $H_2O_3P\text{–}(CH_2)_n\text{–}PO_3H_2$ are increasingly used in the synthesis of hybrid materials based on POMs, owing to their versatile coordination chemistry and the good stability of P–C bond. $\{(Mo_2O_4)(O_3PCH_2PO_3)\}_n$ (n = 3, 4, 10),[15a] $\{Mo_7O_{16}(O_3PCH_2PO_3)_3\}$,[15b] $\{(Mo_2O_4)(O_3PCH_2PO_3)\}$,[15c] $\{Mo_2O_5(O_3PCH_2CH_2PO_3)\}$,[15d] $\{Mo_5O_{15}(O_3PCH_2CH_2PO_3)\}$,[15e] $\{Mo_5O_{15}(O_3PCH_2CH_2CH_2PO_3)\}$,[15f,15g] $[Mo_5O_{15}\{O_3P(CH_2)_nPO_3\}]^{4-}$ (n = 2–6 (ref. 15*h*) and 9 (ref. 15*i*)) and $\{Mo_6O_{18}\{O_3P(CH_2)_5PO_3\}$[15i] are the examples that have been reported. That is to say, it can not only bind to many different metal ions (M) *via* P–O–M bonds, but also possess various potential properties which can be utilized in future.[16]

To the best of our knowledge, only a few analogues of diphosphonate–POMs systems that further functionalized with carboxylic acid ligand have been reported. Herein, the diphosphonate ligand and carboxylic acid ligand synchronously incorporating into POMs grabs our attention. As expected, $(C_3N_2H_5)_4Na[\{(HO_3PCH_2PO_3)Mo_6O_{18}(O_2CC_6H_4OH)_2\}]\cdot(C_3N_2H_4)\cdot 9.5H_2O$ (**1**) constructed by $H_2O_3PCH_2PO_3H_2$ and further modified by *p*-hydroxybenzoic acid has been firstly isolated. $(C_3N_2H_5)_8[\{(HO_3PCH_2PO_3)Mo_6O_{18}(CH_3CO_2)_2\}_2Na_2(H_2O)_2]\cdot 8H_2O$ (**2**) has been discovered with acetic acid instead of *p*-hydroxybenzoic acid. To further study the nature effect of carboxylic acid ligands in this area, malonic acid was used to assembly polyoxomolybdate. Under the conventional solution conditions, another novel "S-shaped" structure compound $(C_3N_2H_5)_8Na_4[\{(O_3PCH_2PO_3)(Mo_6O_{18}(H_2O)_2)(O_2CCH_2CO_2)\}_2(Mo_2O_5)_2(\mu_3\text{-}O)_2]\cdot 14H_2O$ (**3**) with a centre of inversion has been successfully synthesized.

Key Laboratory of Polyoxometalate Chemistry of Henan Province, Institute of Molecular and Crystal Engineering, College of Chemistry and Chemical Engineering, Henan University, Kaifeng 475004, Henan, China. E-mail: jpwang@henu.edu.cn; jyniu@henu.edu.cn; Fax: +86-371-23886876

† Electronic supplementary information (ESI) available: IR spectra of **1–3** and carboxylic acid ligands (Fig. S1). XPRD patterns of **1–3** (Fig. S2). The UV-vis spectra of **1–3** (Fig. S3). ^{31}P NMR spectroscopic characterization of **1–3** with time and $H_2O_3PCH_2PO_3H_2$ (Fig. S4). Thermogravimetric analyses of **1–3** (Fig. S5). The bond valence sum calculations of Mo, P and O atoms on POM fragments in **1–3** (Fig. S6, Table S1, Table S2, Table S3 and Table S4). The coordination environment of P1 and P2 atoms in **1–3** (Fig. S7). Some other supporting figures (Fig. S8–S10) and Table S5. CCDC 1030525, 1030526 and 1030527. For ESI and crystallographic data in CIF or other electronic format see DOI: 10.1039/c5ra01955a

Experimental

Materials and methods

All chemical reagents were commercially purchased and used without any further purification. Elemental analyses (C, H, N) were performed on a Perkin-Elmer 2400-II CHNS/O analyzer. IR spectra were obtained on a Bruker VERTEX 70 IR spectrometer (using KBr pellets) in the range of 4000–400 cm^{-1}. UV-vis absorption spectra were determined on a U-4100 spectrometer at room temperature. Thermogravimetric analyses (TG) were carried out under the nitrogen gas atmosphere on a Mettler-Toledo TGA/SDTA851[e] instrument from 25 to 900 °C with a heating rate of 10 °C min^{-1}. XRPD measurements were performed on a Bruker AXS D8 Advance diffractometer instrument with Cu K_α radiation ($\lambda = 1.54056$ Å) in the angular range $2\theta =$ 10–40° at 293 K. ^{31}P NMR spectra were detected in 5 mm tubes with ^{1}H decoupling on a Bruker AV-400 model spectrometer operating at 400 MHz. ^{31}P chemical shifts were referenced to the 85% H_3PO_4 as external standard.

Synthesis of 1. $Na_2MoO_4 \cdot 2H_2O$ (0.73 g, 3.02 mmol) and *p*-hydroxybenzoic acid (0.14 g, 1.01 mmol) were dissolved in water (10 mL), and $H_2O_3PCH_2PO_3H_2$ (0.08 g, 0.45 mmol) and imidazole (0.13 g, 1.91 mmol) were added. The pH value was adjusted to 4.6 by 2 mol L^{-1} HCl. Then the solution was stirred approximately 2 h at 70 °C. After cooling to room temperature, the solution was filtered and the filtrate was left in an open beaker at room temperature. Colourless block crystals of **1** were obtained after about one month. Yield: 0.19 g (22% based on $H_2O_3PCH_2PO_3H_2$). Elemental analysis (%) calcd for **1**: C, 19.06; H, 3.41; N, 7.41. Found: C, 19.54; H, 3.18; N, 7.24. The following abbreviations for selected IR (KBr, cm^{-1}) were used to assign the peak intensities: s, strong; m, medium; w, weak. 3147 (s), 2849 (m), 1595 (s), 1536 (s), 1400 (s), 1275 (w), 1248 (w), 1170 (w), 1051 (s), 929 (s), 894 (s), 788 (m), 665 (s), 626 (s), 525 (m), 452 (w), 428 (w).

Synthesis of 2. The procedure for the formation of **1** was employed but with NaAc (0.25 g, 3.05 mmol) instead of *p*-hydroxybenzoic acid (0.14 g, 1.01 mmol) and the pH value was adjusted to 4.7 by glacial acetic acid. Yield: 0.33 g (48% based on $H_2O_3PCH_2PO_3H_2$). Elemental analysis (%) calcd for **2**: C, 13.22; H, 2.55; N, 7.26. Found: C, 13.19; H, 2.21; N, 7.43. Selected IR (KBr, cm^{-1}): 3145 (s), 2981 (m), 2845 (m), 2628 (w), 1557 (s), 1426 (s), 1153 (w), 1052 (s), 932 (s), 898 (s), 757 (m), 661 (s), 522 (w), 453 (w), 431 (w).

Synthesis of 3. The procedure for the formation of **1** was employed but with malonic acid (0.21 g, 2.02 mmol) instead of *p*-hydroxybenzoic acid (0.14 g, 1.01 mmol) and the pH value was adjusted to 4.0 by 2 mol L^{-1} HCl. Yield: 0.10 g (14% based on $H_2O_3PCH_2PO_3H_2$). Elemental analysis (%) calcd for **3**: C, 10.06; H, 2.22; N, 5.87. Found: C, 10.33; H, 2.50; N, 5.63. Selected IR (KBr, cm^{-1}): 3149 (s), 2991 (m), 2860 (m), 1584 (s), 1445 (w), 1420 (w), 1370 (m), 1279 (w), 1169 (w), 1079 (s), 1049 (m), 974 (m), 929 (s), 900 (s), 671 (s), 624 (m), 522 (m), 444 (w), 420 (w).

Table 1 Crystal data and structure refinement for compounds **1–3**

	1	**2**	**3**
Empirical formula	$C_{30}H_{56}Mo_6N_{10}NaO_{39.5}P_2$	$C_{34}H_{78}Mo_{12}N_{16}Na_2O_{66}P_4$	$C_{32}H_{84}Mo_{16}N_{16}Na_4O_{86}P_4$
Formula weight	1849.42	3088.26	3819.96
T (K)	293(2)	296(2)	296(2)
Space group	$P\bar{1}$	$P\bar{1}$	$P\bar{1}$
Crystal system	Triclinic	Triclinic	Triclinic
a/Å	12.725(3)	12.5484(9)	12.5891(9)
b/Å	13.292(3)	15.8024(12)	14.2538(10)
c/Å	20.645(4)	15.9316(11)	14.8335(10)
α/deg	90.526(3)	81.1310(10)	84.5250(10)
β/deg	103.738(3)	71.3690(10)	83.8700(10)
γ/deg	111.016(3)	74.8680(10)	80.4970(10)
V/Å^3	3149.2(12)	2881.1(4)	2602.0(3)
Z	2	1	1
Cryst size (mm^3)	0.50 × 0.35 × 0.11	0.45 × 0.32 × 0.24	0.49 × 0.41 × 0.33
D_c/g cm^{-3}	1.950	1.780	2.430
μ/mm^{-1}	1.321	1.415	2.061
F(000)	1830	1508	1840
Limiting indices	$-13 \le h \le 15$	$-14 \le h \le 14$	$-14 \le h \le 14$
	$-15 \le k \le 15$	$-17 \le k \le 18$	$-16 \le k \le 16$
	$-24 \le l \le 24$	$-18 \le l \le 18$	$-17 \le l \le 15$
For data collection/deg	1.80–25.00	2.44–25.00	1.39–25.00
Reflections collected/unique	15 964/10 961	14 731/10 047	13 543/9043
$R_{(int)}$	0.0264	0.0135	0.0200
Goodness-of-fit on F^2	1.007	1.092	1.054
Final R indices	$R_1 = 0.0485$	$R_1 = 0.0370$	$R_1 = 0.0360$
$[I > 2\sigma(I)]$	$wR_2 = 0.1353$	$wR_2 = 0.1276$	$wR_2 = 0.0876$
R indices (all data)	$R_1 = 0.0645$	$R_1 = 0.0443$	$R_1 = 0.0498$
	$wR_2 = 0.1445$	$wR_2 = 0.1331$	$wR_2 = 0.0929$

X-ray crystallography

A summary of crystal data and structure refinements for **1–3** were listed in Table 1. X-ray structure analysis on single crystal was performed at room temperature on a Bruker Apex-II CCD diffractometer with graphite-monochromated Mo K_α radiation ($\lambda = 0.71073$ Å). The crystal data were solved by direct methods and further refined by full-matrix least-squares refinements on F^2 using the SHELXL-97 software and an absorption correction was performed using the SADABS program.[17]

Routine Lorentz and polarization corrections were applied at the same time. All non-hydrogen atoms were refined anisotropically. All hydrogen atoms were positioned geometrically and were not included in the refinements.

Results and discussion

Structural descriptions

Single crystal X-ray diffraction indicates that compounds **1–3** crystallize in the triclinic $P\bar{1}$ space group. Bond valence sum calculations (BVS)[18] indicate that all Mo atoms are in +6 oxidation state and P atoms are in +3 oxidation state in **1–3**. Considering the charge balance of **1–3**, some protons need to be added. To locate the positions of these protons, BVS of all the O atoms on POMs fragments are carried out (Section 6 in ESI†).

The polyanion $[(O_3PCH_2PO_3)Mo_6O_{18}(H_2O)]^{4-}$ that has been reported by Kortz and co-workers[19] can be regarded as the motif of compounds **1–3**. Both compounds **1** and **2** include the $\{(HO_3PCH_2PO_3)Mo_6O_{22}\}$ unit (Fig. 1a), which is composed of a central heteroatom P surrounded by a ring of six $\{MoO_6\}$ octahedra sharing corners and edges alternately. One P from $H_2O_3PCH_2PO_3H_2$ as the central heteroatom is located slightly above the $\{Mo_6\}$ plane (Fig. S8†) and coordinates to three μ_3-O atoms and a C atom, which leads to a trigonal-pyramidal coordination geometry. The other P atom is bond to two edge-sharing $\{MoO_6\}$ octahedra above the $\{Mo_6\}$ plane. As we known, the reported examples $[(CH_3COO)[N(CH_2P\text{-}O_3)_3]Mo_6O_{17}(OH)]^{6-}$ and $\{XMo_6O_{21}\}$ (X = As^{III}, Sb^{III}, Bi^{III}, Se^{IV}, and Te^{IV})[20,21] are modified either with only one carboxylic acid fragment or with the same amino acid species. However, a major feature of **1a** is that the six terminal oxygen atoms above the $\{Mo_6\}$ plane are occupied by two *p*-hydroxybenzoic acid molecules and one $H_2O_3PCH_2PO_3H_2$ fragment. More specifically, both the two *p*-hydroxybenzoic acid molecules are bonded to two edge-sharing $\{MoO_6\}$ octahedra by their {COO} groups on the same side of the ring (Fig. 1b) and the two $\{O_2CC_6H_4OH\}$ groups are almost perpendicular to the $\{Mo_6\}$ plane. Further, the center P atom with the lone pair of electrons is orientated in the same direction with the *p*-hydroxybenzoic acid ligand.

Polyanion **2a** is a reverse symmetrical "crown-type" structure composed of two $\{(HO_3PCH_2PO_3)Mo_6O_{18}(CH_3CO_2)_2\}$ (Fig. 2d) subunits and a linking bridge (Na–O(1W)–Na). The subunit $\{(HO_3PCH_2PO_3)Mo_6O_{18}(CH_3CO_2)_2\}$ could be considered as the participation in assembly with acetic acid based on the basic building block $\{(HO_3PCH_2PO_3)Mo_6O_{22}\}$ (Fig. 2b), which is formed from molybdenum-oxide cluster modified by $H_2O_3PCH_2PO_3H_2$. The six-coordinate center Na1 in **2a** (Fig. 3), which exhibits distorted triangular prism coordination geometry are defined by O3, O12, O17 and O27 from the subunit $\{(HO_3PCH_2PO_3)Mo_6O_{18}(CH_3CO_2)_2\}$ and O1W and O1WA (A: $2-x$, $1-y$, $1-z$) from crystal water molecules [Na–O: 2.357(4)–2.581(4) Å]. Polyanion **3a** appears an "S-shaped" structure with a centre of inversion (Fig. 1d), which is constituted by two $\{(O_3PCH_2PO_3)(Mo_6O_{18}(H_2O)_2)(O_2CCH_2CO_2)(Mo_2O_7)\}$ (Fig. S9†). The $\{Mo_2O_{10}\}$ linker is coordinated to the basic building block $\{(O_3PCH_2PO_3)(Mo_6O_{18}(H_2O)_2)\}$ by O28 from $H_2O_3PCH_2PO_3H_2$ ligand and O31 and O36 from malonic acid molecule. Besides, one {COO} group from malonic acid links two edge-sharing $\{MoO_6\}$ octahedra from $\{(O_3PCH_2PO_3)(Mo_6O_{18}(H_2O)_2)\}$ framework and the other {COO} group bonds to two edge-sharing $\{MoO_6\}$ octahedra from $\{Mo_4O_{18}\}$ linker (Fig. S10†). BVS values for O15 (O15B, B: $1-x$, $1-y$, $1-z$) and O17 (O17B) above/below the $\{Mo_6\}$ plane of **3a** are 0.242 and 0.266, indicating that they are diprotonated (Fig. S6(c)†).

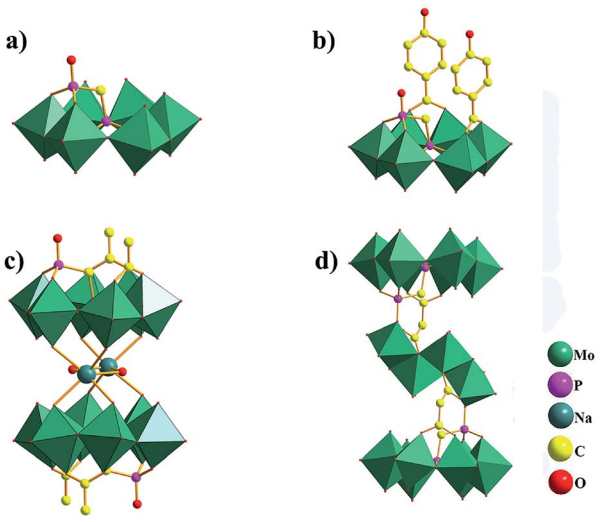

Fig. 1 Polyhedral/ball-and-stick view of the basic building block $\{(HO_3PCH_2PO_3)Mo_6O_{22}\}$ (a); **1a** (b); **2a** (c); **3a** (d). $\{MoO_6\}$, sea green octahedral; hydrogen atoms are omitted for clarity.

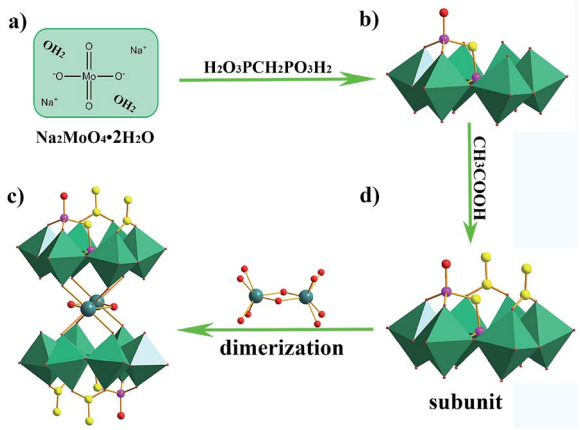

Fig. 2 The schematic stepwise assembly of **2a**.

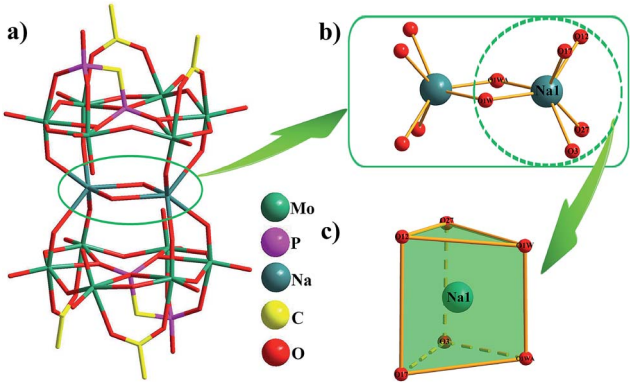

Fig. 3 (a) The sticks representation of polyanion **2a**; (b) ball-and-stick representation of Na–O(1W)–Na bridges; (c) the distorted triangular prism coordination geometry of Na1 in **2a**.

Making a general survey of **1a–3a**, there are two points that worth mentioning. Firstly, both **1a** and **2a** possess two crystallographically unique types of P atoms: P1 exhibits PO_3C tetrahedral geometry [P1–O: 1.517(3)–1.535(3) Å; P1–C: 1.800(5)–1.804(5) Å] residing the apical site in the center of the ring where the basal plane is defined by three μ_3-O atoms and a C atom from $H_2O_3PCH_2PO_3H_2$ ligand; P2 also shows a PO_3C tetrahedral configuration [P2–O: 1.491(4)–1.534(4) Å; P2–C: 1.799(5)–1.812(5) Å] with one C atom from $H_2O_3PCH_2PO_3H_2$ ligand, two μ_2-O atoms and a terminal oxygen atom (O_t). While a little different is that P2 in **3a** is defined by C1, two μ_2-O atoms and a μ_3-O atom [P2–O: 1.519(4)–1.527(4) Å; P2–C1: 1.797(5) Å] (Fig. S7†). Secondly, only two terminal oxygen atoms above/below the $\{Mo_6\}$ plane in $\{(HO_3PCH_2PO_3)Mo_6O_{22}\}$ unit are not shared by *p*-hydroxybenzoic acid for **1a** and acetic acid for **2a**. On the contrary, there are only two terminal oxygen atoms from $\{(O_3PCH_2PO_3)\ (Mo_6O_{18}(H_2O)_2)\}$ unit in **3a** are decorated by malonic acid ligand. The differences may be result from the stereohindrance effect. Compared with **2a**, **3a** is a sandwich-type structure and the sandwich layer $\{Mo_4O_{18}\}$ group is decorated by malonic acid molecule, which possess an "S-shaped" structure. It is proven that using carboxylate ligands to functionalize heteropolymolybdates is feasible. At the same time, this fully shows the profound effect of carboxylic acid ligand in the self-assembly process on constructing POM-based architectures.

Synthesis discussion

To date, the noncovalent POM-based hybrids are well-developed. However, there still remains much research on the hybrids in which the POMs and the organic groups are linked through covalent interactions. A large number of diphosphonate-containing compounds in the literature are insoluble or unstable,[22] while the Mo^{VI} complexes reported here are soluble and stable in aqueous solution as evidenced by ^{31}P NMR spectroscopy. In this paper, carboxylic acid and diphosphate were chosen as ligands, and three compounds were synthesized in the aqueous solution by the one-pot reaction from sodium molybdate. The synthetic routes of compounds **1–3** are shown in Scheme 1. Further, in order to explore the best conditions, we adjusted the solution in terms of pH, counterion, molar ratio and temperature. Table S5† shows a summary of the reaction conditions and the factors affecting are analysed as follows: (a) the counterion is especially important. During the preparation of **1–3**, when using K^+ instead of $[C_3N_2H_5]^+$ as the counterion, no crystals could be obtained. To our knowledge, the reason may be that the larger organic counterion $[C_3N_2H_5]^+$ undergo extensive C–H···O hydrogen bonding interactions with the cluster, which is preferable for the formation of the framework.[23] (b) The molar ratio of Mo/P plays an important role in the composition and yield of the product and the best ratio of Mo/P is 10/3. (c) As it turns out, the reaction temperature between 60 °C and 80 °C has almost no significant effect on the quality of crystals. However, when the reaction temperature keeps below 60 °C, we failed to obtain the pure crystalline phase of compounds **1–3**. (d) The pH value should be controlled in the range of 3.5 to 5.5. We could not obtained good quality crystals when the pH value is lower than 3.5. While the pH value is higher than 5.5, some amorphous precipitates in the course of crystallization are discovered and we filtrated it right now but it did not work to the formation of crystals.

XRPD and FT-IR patterns

The experimental XRPD patterns for **1–3** are in good agreement with the simulated XRPD patterns from the single-crystal X-ray diffraction, demonstrating the good phase purity for **1–3** (Fig. S2†). The differences in intensity between the experimental and simulated XRPD patterns might be due to the variation in preferred orientation of the powder sample during collection of the experimental XRPD.

The peak shapes of the IR spectra of **1–3** (Fig. S1(a)†) show similar features for the skeletal vibrations from 400 to 1700 cm^{-1}, indicating that **1–3** almost have the same basic framework. Meanwhile they are in good agreement with the

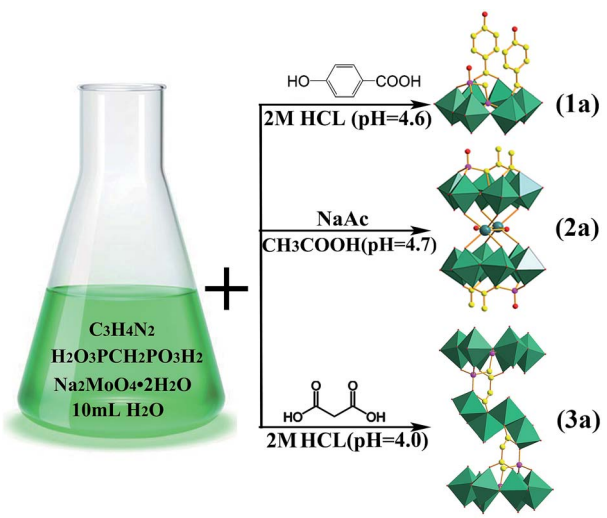

Scheme 1 The synthetic pathways of **1–3** (all of **1–3** were stirred approximately 2 h at 70 °C).

results of single-crystal X-ray structural analyses. The peaks at 929 and 894 cm^{-1}, 932 and 898 cm^{-1}, 929 and 900 cm^{-1} are attributed to the Mo–O_t characteristic vibration for **1**, **2** and **3**, respectively; and the peaks below 815 cm^{-1} assigned to the bridging Mo–O–Mo vibration. The P–O vibrations are seen at 1170 and 1051 cm^{-1} for **1**, 1153 and 1052 cm^{-1} for **2**, and 1169 and 1079 cm^{-1} for **3**, which are respectively assigned to two environment phosphorus. Compared with the IR spectra of the uncoordinated carboxylic acid (1620–1740 cm^{-1}) (Fig. S1(b)†), the vibration bands of **1–3** show obvious red shifts, as a result of the coordination of carboxylic acid ligand with metal ion.[24] In addition, the peaks at 3360–3500 cm^{-1} could be attributed to the characteristic vibrations of hydroxyl from lattice water molecules.

^{31}P NMR spectroscopic characterization of compounds 1–3

NMR spectroscopy is a powerful tool to confirm the structure of polyanions and investigate their stability in solution. To verify the coordination environment of P atoms, the ^{31}P NMR spectra of compounds **1–3** have been explored after they are dissolved in D_2O at room temperature. X-ray analysis reveals that there are two types of P atoms in the three structures. P1 should give one signal and P2 should give another signal. As shown in Fig. S4(d)† and Fig. 4, ^{31}P NMR spectrum of $H_2O_3PCH_2PO_3H_2$ ligand possesses one resonance at 19.05 ppm and the ^{31}P NMR spectra of compounds **1–3** all exhibit two resonances. Indeed, The singles at 17.98 ppm, 17.93 ppm and 18.18 ppm may be attributed to the presence of the central heteroatom P surrounded by a ring of six $\{MoO_6\}$ octahedra for **1**, **2** and **3**, respectively. The resonance peak found at 25.45 ppm for **1**, 25.45 ppm for **2** and 25.30 ppm for **3** can reveal the presence of the other species of P sitting above/below the $\{Mo_6\}$ plane. This result agrees with the aforementioned conclusion by X-ray analysis.

Furthermore, to determine whether the structures characterized in the crystal state are stable in solution, the ^{31}P NMR spectra with time from 0 to 72 h have been researched (Fig. S4†). The two resonances attributed to **1** and **2** have almost no changing suggest the coordination environment of P atoms unchanged with time. For **3**, it shows very slightly shift of the resonance at 18.18 ppm after four hours. Twelve hours later, the two resonances at 25.30 ppm and 18.18 ppm are all slightly shifts that show the slow decomposition of **3**. The ^{31}P NMR spectroscopic studies show that the skeleton of **1** and **2** are stable in aqueous solution at least 72 h.

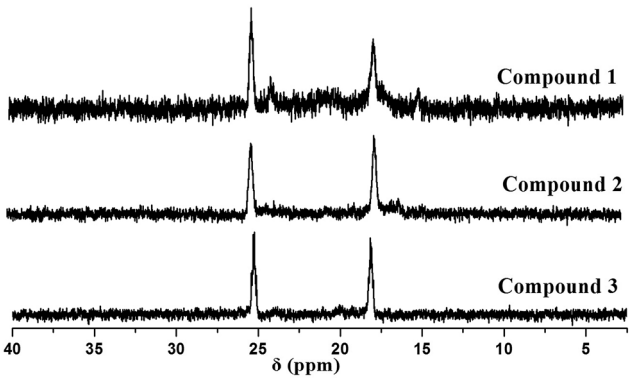

Fig. 4 ^{31}P NMR spectra of **1–3** dissolved in D_2O at room temperature.

Cyclic voltammetric behavior of 1–, 2– and 3–GCEs in aqueous electrolyte

To explore the electrochemical property of compounds **1–3**, cyclic voltammetric (CV) behavior in the range of 0–0.6 V were measured at different scan rates in Na_2SO_4/H_2SO_4 aqueous solution at pH = 1.0 (Fig. 5). The electrochemical behaviors of the **1**–, **2**– and **3**–glassy carbon electrodes (GCEs) are similar except for some slight potential shift and the behavior of **1**–GCE has been taken as an example. As shown in Fig. 5a, two pairs of redox peaks (I–I′, II–II′) are observed of compound **1**. At the scan rate of 250 mV s^{-1}, the CVs of **1**–GCE show the mean peak potentials $E_{1/2} = (E_{pa} + E_{pc})/2$ at +121 mV (I–I′) and +248 mV

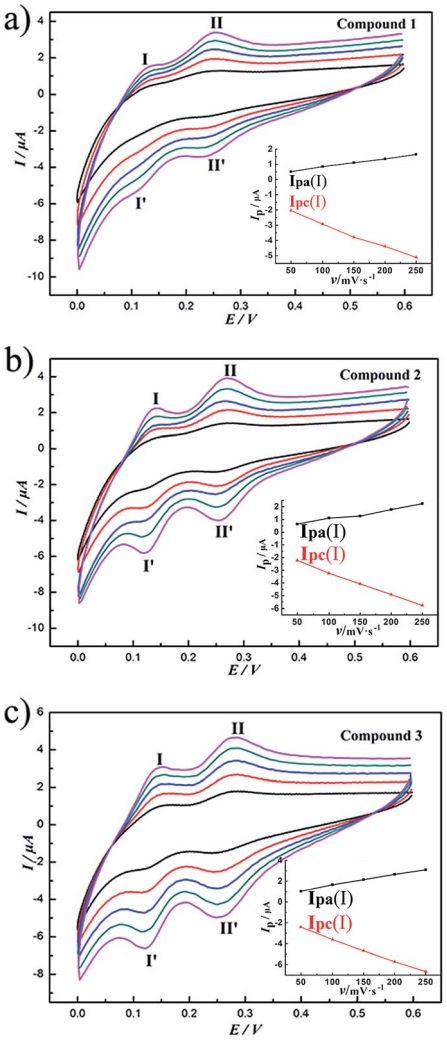

Fig. 5 Cyclic voltammograms of **1–3** (1×10^{-3} mol L^{-1}) under scan rates from inner to outer: 50, 100, 150, 200 and 250 mV s^{-1}; insert figures: the plots of the anodic and the cathodic peak I–I′ currents against scan rates for **1–3**. Working electrode, glassy carbon; reference electrode, SCE.

(II–II′). The half-wave potentials are at +131 mV (I–I′) and +265 mV (II–II′) for **2**–GCE (Fig. 5b), +135 mV (I–I′) and +272 mV (II–II′) for **3**–GCE (Fig. 5c), respectively. The redox peaks I–I′ and II–II′ can be ascribed to reversible Mo^{VI}/Mo^{V} and Mo^{V}/Mo^{IV} redox reactions. In other words, it is the result from two reversible one-electron processes of Mo atoms.[25] The cathodic peak potentials shift slightly towards negative potential values and the anodic peak potentials shift towards positive potential values with the increasing scan rates from 50 to 250 mV s^{-1}.

In addition, the peak currents are proportional to the scan rate (insert figures in Fig. 5), which indicates that the redox processes are surface-controlled, and the exchanging rate of electrons is fast.[26] These results exhibit almost no structural effect of **1a–3a** on the redox properties, except for some slight potential shifts of the redox peaks.

Conclusions

In this paper, three novel diphosphonate-containing POMs functionalized by carboxylic acid ligand have been isolated. The different structural characterizations of **1a–3a** reveal that the coordinated carboxylate pendants play an important role in the formation of polyanions and show the strong chelating ability of this class as ligand. These results may open a way to the synthesis of a large family of hybrid POMs, which are functionalized with variable diphosphonate and carboxylic acid ligands, synchronously. The following work we will focus on synthesizing and further investigating more multidimensional hybrids diphosphonate–POMs by means of introducing different POMs framework or other organic ligands.

Acknowledgements

We gratefully acknowledge financial support from the Natural Science Foundation of China, the Natural Science Foundation of Henan Province for financial support.

Notes and references

1 (*a*) D. L. Long, E. Burkholder and L. Cronin, *Chem. Soc. Rev.*, 2007, **36**, 105; (*b*) M. T. Pope and A. Müller, *Angew. Chem., Int. Ed.*, 1991, **30**, 34–48.

2 (*a*) A. Proust, R. Thouvenot and P. Gouzerh, *Chem. Commun.*, 2008, 1837; (*b*) A. Dolbecq, E. Dumas, C. R. Mayer and P. Mialane, *Chem. Rev.*, 2010, **110**, 6009.

3 J. D. Compain, P. Mialane, A. Dolbecq, I. M. Mbomekallé, J. Marrot, F. Sécheresse, E. Rivière, G. Rogez and W. Wernsdorfer, *Angew. Chem., Int. Ed.*, 2009, **48**, 3077.

4 (*a*) E. Coronado and C. J. Gómez-García, *Chem. Rev.*, 1998, **98**, 273; (*b*) Y. F. Song and R. Tsunashima, *Chem. Soc. Rev.*, 2012, **41**, 7384.

5 J. T. Rhule, C. L. Hill and D. A. Judd, *Chem. Rev.*, 1998, **98**, 327.

6 D. L. Long, R. Tsunashima and L. Cronin, *Angew. Chem., Int. Ed.*, 2010, **49**, 1736.

7 J. Y. Niu, G. Chen, J. W. Zhao, P. T. Ma, S. Z. Li, J. P. Wang, M. X. Li, Y. Bai and B. S. Ji, *Chem.–Eur. J.*, 2010, **16**, 7082.

8 L. Xu, M. Lu, B. B. Xu, Y. G. Wei, Z. H. Peng and D. R. Powell, *Angew. Chem., Int. Ed.*, 2002, **41**, 4129.

9 (*a*) A. Proust, R. Thouvebot and P. Gouzerh, *Chem. Commun.*, 2008, 1837; (*b*) J. Hao, Y. Xia, L. Wang, L. Ruhlmann, Y. Zhu, Q. Li, P. Yin, Y. Wei and H. Guo, *Angew. Chem., Int. Ed.*, 2008, **47**, 2626.

10 (*a*) G. G. Gao, L. Xu, X. S. Qu, H. Liu and Y. Y. Yang, *Inorg. Chem.*, 2008, **47**, 3402; (*b*) Z. H. Zhou, S. Y. Hou, Z. X. Cao, K. R. Tsai and Y. L. Chow, *Inorg. Chem.*, 2006, **45**, 8447; (*c*) W. B. Yang, C. Z. Lu, X. Lin and H. H. Zhuang, *Inorg. Chem.*, 2002, **41**, 452; (*d*) G. Liu, S. W. Zhang and Y. Q. Tang, *Dalton Trans.*, 2002, 2036; (*e*) C. D. Peloux, P. Mialane, A. Dolbecq, J. Marrot and F. Sécheresse, *Angew. Chem., Int. Ed.*, 2002, **41**, 2808.

11 G. H. Sima, Q. Li, Y. Zhu, C. L. Lv, R. N. N. Khan, J. Hao, J. Zhang and Y. G. Wei, *Inorg. Chem.*, 2013, **52**, 6551.

12 B. J. S. Johnson, R. C. Schroden, C. C. Zhu and A. Stein, *Inorg. Chem.*, 2001, **40**, 5972.

13 (*a*) B. Modec, D. Dolenc and M. Kasunič, *Inorg. Chem.*, 2008, **47**, 3625; (*b*) B. Modec, D. Dolenc, J. V. Brenčič, J. Koller and J. Zubieta, *Eur. J. Inorg. Chem.*, 2005, 3224; (*c*) B. Modec, J. V. Brenčič, E. M. Burkholder and J. Zubieta, *DaltonTrans.*, 2003, 4618; (*d*) B. Modec, J. V. Brenčič, D. Dolenc and J. Zubieta, *Dalton Trans.*, 2002, 4582.

14 (*a*) J. F. Lemonnier, A. Kachmar, S. Floquet, J. Marrot, M.-M. Rohmer, M. Bénard and E. Cadot, *Dalton Trans.*, 2008, 4565; (*b*) J.-F. Lemonnier, S. Floquet, J. Marrot, E. Terazzi, C. Piguet, P. Lesot, A. Pinto and E. Cadot, *Chem.–Eur. J.*, 2007, **13**, 3548; (*c*) J.-F. Lemonnier, S. Floquet, A. Kachmar, M.-M. Rohmer, M. Bénard, J. Marrot, E. Terazzi, C. Piguet and E. Cadot, *Dalton Trans.*, 2007, 3043; (*d*) B. Salignac, S. Riedel, A. Dolbecq, F. Sécheresse and E. Cadot, *J. Am. Chem. Soc.*, 2000, **122**, 10381.

15 (*a*) C. D. Peloux, A. Dolbecq, P. Mialane, J. Marrot and F. Sécheresse, *Dalton Trans.*, 2004, 1259; (*b*) E. Dumas, C. Sassoye, K. D. Smith and S. C. Sevov, *Inorg. Chem.*, 2002, **41**, 4029; (*c*) A. Dolbecq, L. Lisnard, P. Mialane, J. Marrot, M. Bénard, M. M. Rohmer and F. Sécheresse, *Inorg. Chem.*, 2006, **45**, 5898; (*d*) K. P. Rao, V. Balraj, M. P. Minimol and K. Vidyasagar, *Inorg. Chem.*, 2004, **43**, 4610; (*e*) E. Burkholder, V. Golub, C. J. O'Connorb and J. Zubieta, *Chem. Commun.*, 2003, 2128; (*f*) R. C. Finn, R. S. Rarig and J. Zubieta, *Inorg. Chem.*, 2002, **41**, 2109; (*g*) R. C. Finn and J. Zubieta, *Inorg. Chem.*, 2001, **40**, 2466; (*h*) N. G. Armatas, W. Ouellette, K. Whitenack and J. Zubieta, *Inorg. Chem.*, 2009, **48**, 8897; (*i*) N. G. Armatas, D. G. Allis, A. Prosvirin, K. Dunbar and J. Zubieta, *Inorg. Chem.*, 2008, **47**, 832.

16 (*a*) C. R. Mayer, M. Hervé, H. Lavanant, J.-C. Blais and F. Sécheresse, *Eur. J. Inorg. Chem.*, 2004, 973; (*b*) E. Dumas, C. Sassoye, K. D. Smith and S. C. Sevov, *Inorg. Chem.*, 2002, **41**, 4029; (*c*) R. C. Finn, E. Burkholder and J. Zubieta, *Chem. Commun.*, 2001, 1852; (*d*) A. Banerjee, B. S. Bassil, G.-V. Röschenthaler and U. Kortz, *Chem. Soc. Rev.*, 2012, **41**, 7590.

17 G. M. Sheldrick, SHELXL97, *Program for Crystal Structure Refinement*, University of Göttingen, Göttingen, Germany,

1997; G. M. Sheldrick, SHELXL97, *Program for Crystal Structure Solution*, University of Göttingen, Göttingen, Germany, 1997.

18 I. D. Brown and D. Altermatt, *Acta Crystallogr.*, 1985, **B41**, 244.

19 U. Kortz and M. T. Pope, *Inorg. Chem.*, 1995, **34**, 2160.

20 L. Yang, Z. Zhou, P. T. Ma, J. P. Wang and J. Y. Niu, *CrystEngComm*, 2013, **15**, 5452.

21 U. Kortz, M. G. Savelieff, F. Y. A. Ghali, L. M. Khalil, S. A. Maalouf and D. I. Sinno, *Angew. Chem., Int. Ed.*, 2002, **41**, 4070.

22 J. D. Compain, P. Mialane, J. Marrot, F. Sécheresse, W. Zhu, E. Oldfield and A. Dolbecq, *Chem.–Eur. J.*, 2010, **16**, 13741.

23 C. P. Pradeep, D. L. Long and L. Cronin, *Dalton Trans.*, 2010, **39**, 9443.

24 B. Modec, D. Dolenc and M. Kasunič, *Inorg. Chem.*, 2008, **47**, 3625.

25 (*a*) H. Jin, Y. F. Qi, E. B. Wang, Y. G. Li, C. Qin, X. L. Wang and S. Chang, *Eur. J. Inorg. Chem.*, 2006, 4541; (*b*) C. Qin, X. L. Wang, Y. F. Qi, E. B. Wang, C. W. Hu and L. Xu, *J. Solid State Chem.*, 2004, **177**, 3263.

26 G. S. Yang, H. Y. Zang, Y. Q. Lan, X. L. Wang, C. J. Jiang, Z. M. Su and L. D. Zhu, *CrystEngComm*, 2011, **1s3**, 1461.